Wind and Structures, Vol. 1, No. 2 (1998) 175-181
DOI: http://dx.doi.org/10.12989/was.1998.1.2.175

Role of coupled derivatives on flutter instabilities

Masaru Matsumoto† and Kazuhiro Abe‡

Department of Global Environment Engineering, Kyoto University, Japan

Abstract. Torsional flutter occurs at 2D rectangular cylinders with side ratios *B/D* smaller than about 8 or 10. On the other hand, slender cylinders indicate the occurrence of coupled flutter, which means the coupled derivatives of slender cylinders have more significant role for flutter instability than that of bluffer ones. In this paper, based upon so called "Step-by-step analysis", it is clarified the coupled derivatives stabilize torsional flutter instability of bluffer cylinders (e.x. *B/D*=5), while they destabilize torsional flutter or coupled flutter instabilities of more slender cylinders. The boundary of them exists between *B/D*=5 and 8.

Key words: flutter instabilities; coupled derivatives.

1. Introduction

The onset of flutter causes directly for structural failure, therefore flutter stabilization should be carefully considered for the design of super-long spanned bridges. The clarification of flutter mechanism is, still nowadays, one of the major problems in the field of wind engineering. Flutter instabilities are generally discussed based upon the aerodynamic derivatives. In this paper, mainly the important role of coupled derivatives is explained by "Step-by-Step Analysis". The aim of this study is clarification of the contribution of coupled term on torsional flutter instability of bluffer 2D rectangular cylinders.

2. Aerodynamic derivatives

Considering the unsteady lift force and the pitching moment per unit length, the following equations for heaving-torsional 2DOF system proposed by Scanlan (1971) are widely adopted :

$$L = \frac{1}{2}\rho(2b)U^2\left\{kH_1^*\frac{\dot{\eta}}{U}+kH_2^*\frac{b\dot{\phi}}{U}+k^2H_3^*\phi+k^2H_4^*\frac{\eta}{b}\right\}$$

$$M = \frac{1}{2}\rho(2b^2)U^2\left\{kA_1^*\frac{\dot{\eta}}{U}+kA_2^*\frac{b\dot{\phi}}{U}+k^2A_3^*\phi+k^2A_4^*\frac{\eta}{b}\right\}$$

† Professor
‡ Graduate Student

where L, M : unsteady lift force and pitching moment per unit length, η, ϕ : heaving and torsional displacement, ρ : air density, b : half chord length ($=B/2$), U : wind velocity, k : reduced frequency ($=b\omega/U$, ω : circular frequency at a certain velocity, U)

Here, a torsional damping term, A_2^*, is a measure for the torsional flutter appearance, and its positive and negative value correspond to the aerodynamic instability and stability to torsional flutter, respectively. On the other hand, the coupled aerodynamic derivatives H_2^*, H_3^*, A_1^*, A_4^* have a significant role for flutter instabilities in 2DOF vibration modes.

Aerodynamic derivatives of 2D rectangular cylinders (Fig. 1) with the range of side-ratio B/D from 5 to 20 are illustrated in Fig. 2 (Matsumoto, Niihara and Kobayashi 1994). This figure shows torsional flutter occurs at the range of B/D=5 to 10 where the value of A_2^* has positive values, and A_2^* decreases with the increase of B/D.

The aerodynamic derivatives can be, also, obtained from integrating the unsteady pressure coefficient $\tilde{C}p$ and the phase lag Ψ between the cylinder motion and unsteady pressure as followings :

$$H_1^* = \frac{-U^2}{2b\omega^2\eta_0}\int_{-1}^{1} \tilde{C}_p \cos\Psi_B \, dx = \frac{U^2}{2b\omega^2\eta_0}\int_{-1}^{1} \tilde{C}_{pH_1^*} \, dx$$

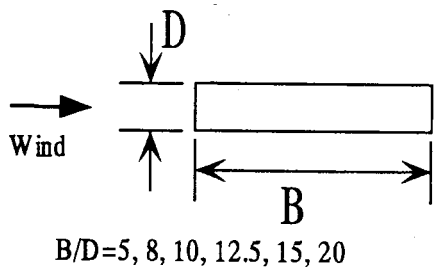

Fig. 1 2D rectangular cylinders

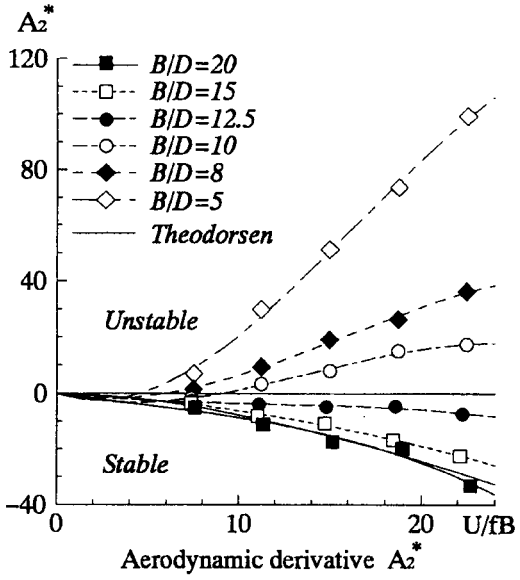

Fig. 2 Aerodynamic derivative A_2^* for 2D rectangular cylinders [B/D=5, 8, 10, 12.5, 15, 20]

$$H_2^* = \frac{U^2}{2b^2\omega^2\phi_0}\int_{-1}^{1} \widetilde{C}_p \sin\Psi_T\, dx = \frac{U^2}{2b^2\omega^2\phi_0}\int_{-1}^{1} \widetilde{C}_{pH_2^*}\, dx$$

$$H_4^* = \frac{-U^2}{2b\,\omega^2\eta_0}\int_{-1}^{1} \widetilde{C}_p \sin\Psi_B\, dx = \frac{U^2}{2b\,\omega^2\eta_0}\int_{-1}^{1} \widetilde{C}_{pH_4^*}\, dx$$

$$H_3^* = \frac{-U^2}{2b^2\omega^2\phi_0}\int_{-1}^{1} \widetilde{C}_p \cos\Psi_T\, dx = \frac{U^2}{2b^2\omega^2\phi_0}\int_{-1}^{1} \widetilde{C}_{pH_3^*}\, dx$$

$$A_1^* = \frac{-U^2}{2b\,\omega^2\eta_0}\int_{-1}^{1} \widetilde{C}_p\, x\cos\Psi_B\, dx = \frac{U^2}{2b\,\omega^2\eta_0}\int_{-1}^{1} \widetilde{C}_{pA_1^*}\, dx$$

$$A_2^* = \frac{U^2}{2b^2\omega^2\phi_0}\int_{-1}^{1} \widetilde{C}_p\, x\sin\Psi_T\, dx = \frac{U^2}{2b^2\omega^2\phi_0}\int_{-1}^{1} \widetilde{C}_{pA_2^*}\, dx$$

$$A_4^* = \frac{-U^2}{2b\,\omega^2\eta_0}\int_{-1}^{1} \widetilde{C}_p\, x\sin\Psi_B\, dx = \frac{U^2}{2b\,\omega^2\eta_0}\int_{-1}^{1} \widetilde{C}_{pA_4^*}\, dx$$

$$A_3^* = \frac{-U^2}{2b^2\omega^2\phi_0}\int_{-1}^{1} \widetilde{C}_p\, x\cos\Psi_T\, dx = \frac{U^2}{2b^2\omega^2\phi_0}\int_{-1}^{1} \widetilde{C}_{pA_3^*}\, dx$$

where η_0, ϕ_0 : amplitude of 1DOF heaving/torsional motion.

Unsteady pressure and phase lag distributions of rectangular cylinders with side-ratios B/D= 5 to 20 under 1DOF torsional forced vibration are shown in Fig. 3 (Matsumoto, Daito, Yoshizumi and Ichikawa 1997). In Fig. 3, $\widetilde{Cp}$, and ϕ is plotted against the non-dimensionalized coordinate by the cylinder thickness, that is x/D. These figures clarify both amplitude and phase properties of pressures are fundamentally identical from the point of chord-wise distribution. This fact means the after body length of these cylinders have less effect on pressure characteristics around the body surface, which are caused by the local flow separation near the leading edge and flow reattachment.

The aerodynamic derivative A_2^* can be, also, associated with $\widetilde{Cp}_{H_2^*}$ as follows :

$$A_2^* = \frac{U^2}{2b^2\omega^2\phi_0}\int_{-1}^{1} \widetilde{C}_p \cdot x \cdot \sin\theta dx = \frac{U^2}{2b^2\omega^2\theta_0}\int_{-1}^{1} x \cdot \widetilde{C}_{pH_2^*}\, dx = \frac{x_G\, U^2}{2b^2\omega^2\phi_0}\int_{-1}^{1} \widetilde{C}_{pH_2^*}\, dx\ ,$$

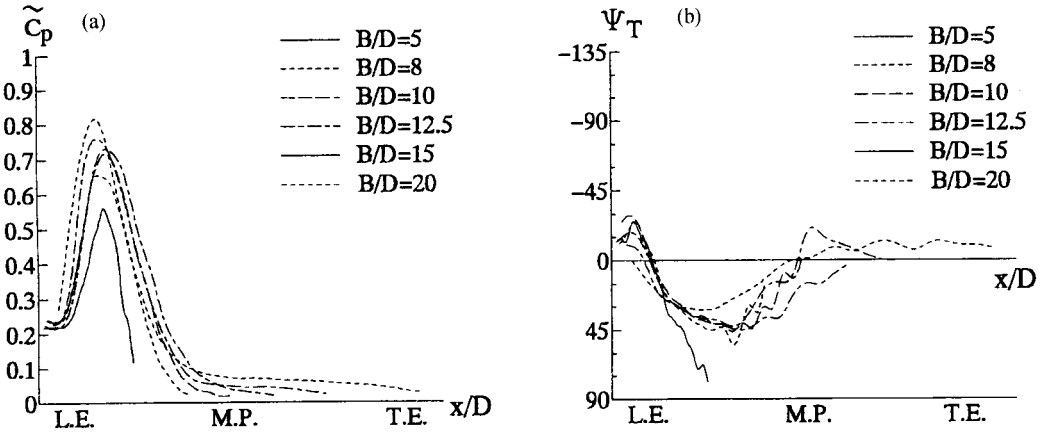

Fig. 3 Unsteady pressure distributions (U/fB=18.7) : (a) unsteady pressure coefficient and (b) phase lag

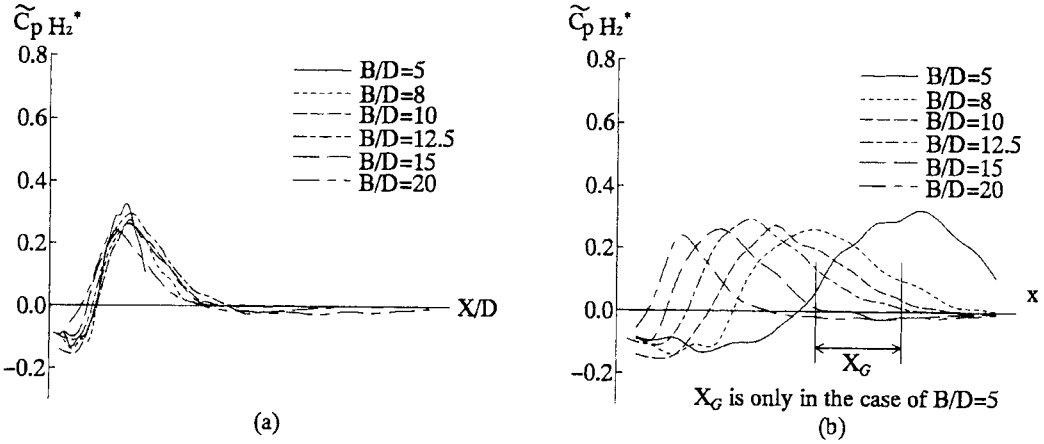

Fig. 4 Torsional flutter instability for 2D rectangular cylinders (U/fD=18.52) (a) : analogy of unsteady pressure (b) : unsteady pressure

where

$$\widetilde{C}_{pH_2^*} = \widetilde{C}_p \cdot \sin\theta, \quad \left(H_2^* = \frac{U^2}{2b^2\omega^2\phi_0} \int_{-1}^{1} \widetilde{C}_p \sin\theta dx \right)$$

x_G is the distance of the gravity center of $\widetilde{Cp}_{H_2}*$ distribution from the mid-chord point, $x=X/b$ (X : the distance from the mid-chord point, x=-1 : leading edge, x=1 : trailing edge) and ϕ_0 : amplitude of the 1DOF torsional motion.

$\widetilde{Cp}_{H_2}*$ distribution of 2D rectangular cylinders is illustrated in Figs. 4(a), (b), which are plotted against the the non-dimensionalized coordinate by the cylinder thickness, that is x/D, and the half-chord length, that is $x=X/B$, respectively. In Fig. 4(a), the analogy of $\widetilde{Cp}_{H_2}*$ distribution is derived from the unsteady pressure distributions shown in Fig. 3. Therefore, the position of the gravity center of $\widetilde{Cp}_{H_2}*$ distribution of Fig. 4(b) continuously moves from trailing edge side to leading edge side with the increase of B/D, which means the value of A_2^* decreases gradually from positive to negative with increase of B/D. In other words, the mechanism of torsional flutter can be thought to be identical with that of coupled flutter.

3. Step-by-Step Analysis

So called "Step-by-Step Method" is quite useful to investigate the effect of each aerodynamic derivative on the flutter excitation. The flutter property obtained by this method is significantly coincides well to that of the conventional eigenvalue analysis. The process of "Step-by-Step method (for torsional branch)" is illustrated in Fig. 5. In 1DOF torsional mode, the equation of motion under wind load without structural damping is described as follows :

$$\ddot{\phi} + \omega_{\phi 0}^2 \phi = \left(\frac{\rho b^4}{I} \right) \omega_F A_2^* \dot{\phi} + \left(\frac{\rho b^4}{I} \right) \omega_F^2 A_3^* \phi$$

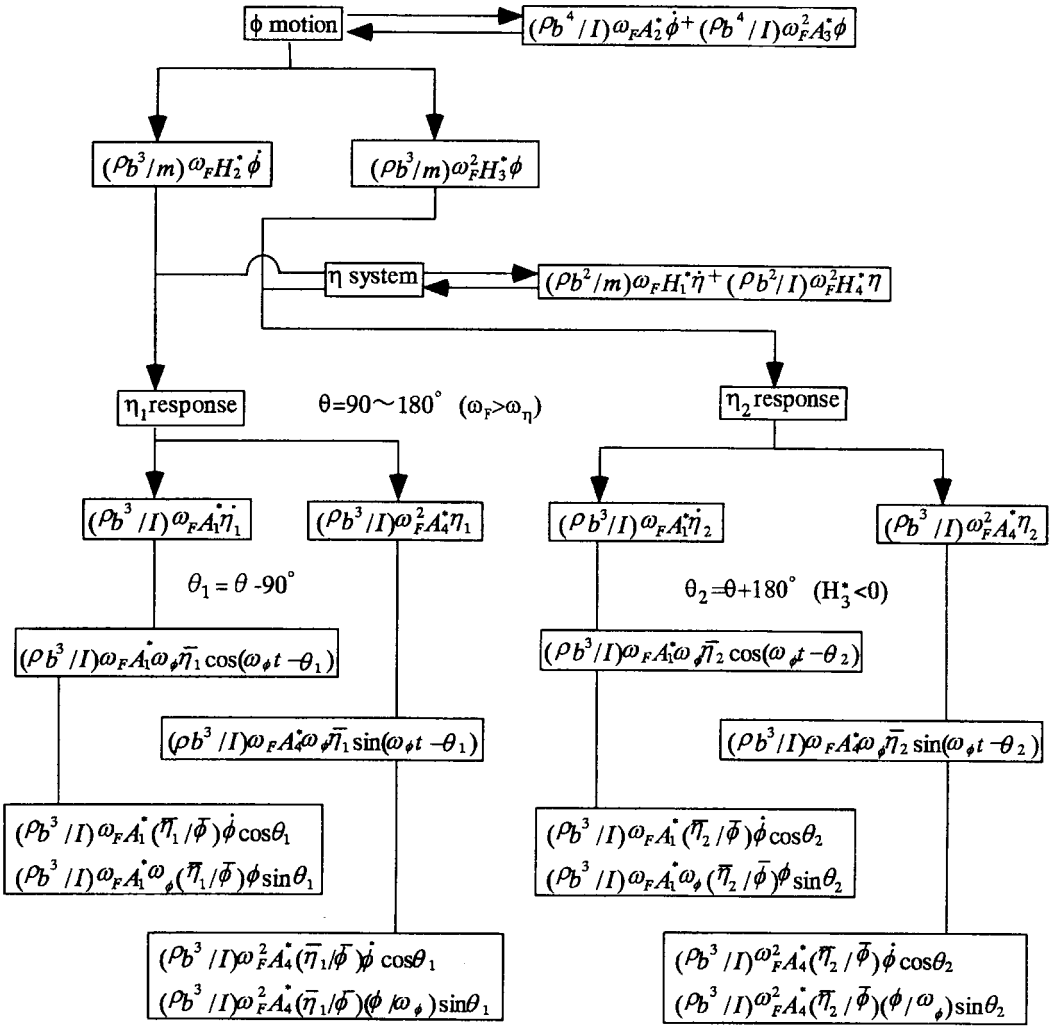

Fig. 5 Flow chart for "Step-by-Step Analysis (torsional branch)"

where ϕ : torsional displacement, $\dot{\phi}$: torsional velocity, $\omega_{\phi 0}$: torsional natural frequency, ω_F : flutter frequency, ρ : air density, b : half-chord length, I : mass inertia per unit length.

Then,

$$\ddot{\phi} + 2\zeta_\phi \omega_\phi \dot{\phi} + \omega_\phi^2 \phi = 0$$

where ω_ϕ : torsional frequency, ζ_ϕ : torsional damping coefficient ($=\delta_\phi / 2\pi$).

Hence, this system wouldn't show divergent torsional motion unless torsional damping coefficient ζ_ϕ, that is determined by A_2^*, has a positive value. Since heaving motion exists in the 2DOF mode, torsional vibration arouses the heaving motion, and this heaving motion causes torsional vibration again. In 2DOF vibration mode, such a feedback system is formulated.

Here, the difference of torsional responses of H-shaped section in 1DOF and 2DOF vibration modes is presented by Karman and Dann (1949), considering on the onset critical reduced wind velocity of flutter (see Fig. 6). In freely suspended system, coupled aerodynamic

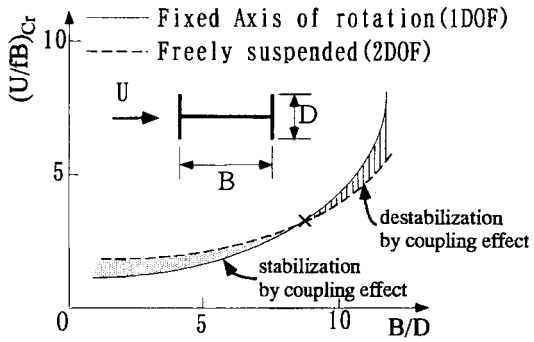

Fig. 6 Critical wind velocity of flutter in torsional mode for 2D H-shaped cylinders (Based on Karman and Dann 1949)

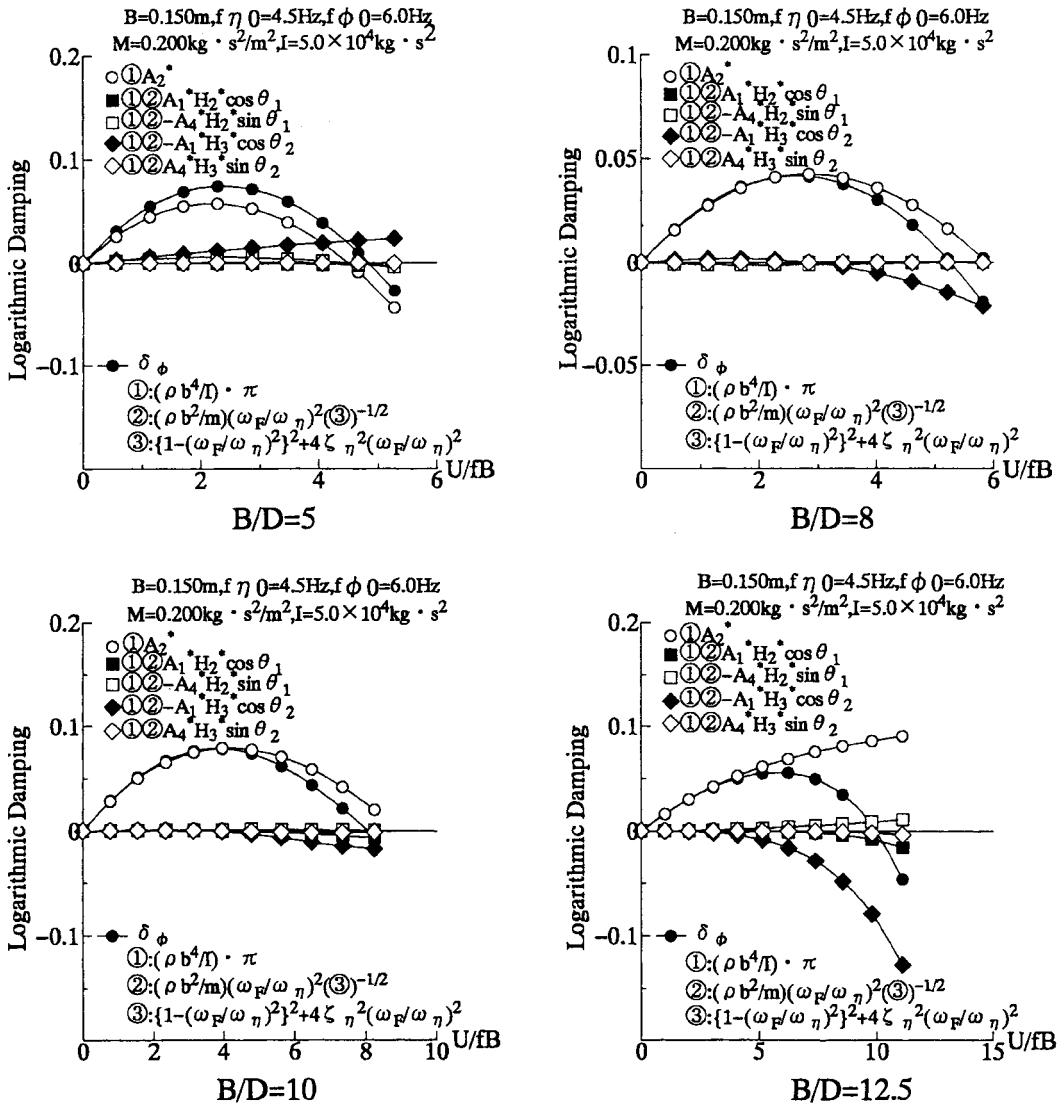

Fig. 7 The role of each aerodynamic derivatives

forces have a significant meaning. In the bluffer H-shaped sections than B/D=9, coupled aerodynamic forces make a large contribution toward the stabilization for torsional flutter instability.

Fig. 7 shows the results of "Step-by-Step Analysis" of the rectangular cylinders. Torsional damping δ(●) can be expressed as the sum of five terms (○ ■ □ ◆ ◇), The zero-crossing point of δ_ϕ represents the onset of flutter. To see Fig. 7, A_2^* (included in ○) stabilize the coupled flutter (B/D=12.5) and destabilize the torsional flutter (B/D=5, 8, 10). The zero-crossing points of ● of B/D=8, 10 are lower than that of ○. This fact means coupled forces still destabilizes torsional flutter instability. On the other hand, ● of B/D=5 is zero-crossed at higher reduced wind velocity mainly because of the positive value of coupled term ◆. This fact is consistent with the result of Karman and Dann (see Fig. 6), that coupled derivatives stabilize torsional flutter of the bluffer H-shaped sections. Though there is a difference of the critical side-ratios between rectangular cylinder and H-shaped section, the difference is agreeable with the fact that H-shaped section shows the aerodynamic property such like that of a more slender rectangular cylinder (Matsumoto 1995).

4. Conclusions

Generally, A_2^* stabilize coupled flutter and destabilize torsional flutter. The boundary between the torsional flutter and coupled flutter exists at side-ratio B/D=10 to 12.5. On the other hand, coupled derivatives stabilize torsional flutter of relatively bluffer cylinders, i.e., B/D=5 but destabilize that of slender ones, i.e., B/D=8, 10. The effect of coupled derivatives on the torsional flutter instabilities changes between the side-ratio B/D=5 and 8. Thus, the coupled aerodynamic forces have a significant part for aerodynamic instabilities. Therefore, the control of this should be discussed well to accomplish the stabilization of flutter instabilities.

Acknowledgements

Finally, the authors would like to express their sincere appreciation to Professor H. Shirato, Dr. X.C. Chen, Dr. T. Yagi of Kyoto University, Y. Niihara of Kajima Corporation and Y. Kobayashi of Miyaji Iron Works Co., Ltd. for their great contribution.

References

Matsumoto, M., Niihara, Y., Kobayashi, Y., (1994), "On mechanism of flutter phenomena for structural sections", **40A**, *Journal of Structural Engineering*.

Matsumoto, M., Daito, Y., Yoshizumi, F., Ichikawa, Y., (1997), "Torsional flutter of bluff bodies", *Journal of Wind Engineering and Industrial Aerodynamics*.

Matsumoto, M. (1995), "Aerodynamic damping of prisms", *Proc. IWEF*.

Scanlan, R.H. and Tomko, J.J. (1971), "Airfoil and bridge deck flutter derivatives", *J. ASCE EM6*.

Von Karman, Th. and Dann, L.G., (1949), "Aerodynamic stability of suspension bridges", F.D. Farquharson(ed.) Bull. of Univ. Washington Eng. Exp. Station, No. 116 Part 3.